

RESEARCH ARTICLE

Open Access



The broad use of the *Pm8* resistance gene in wheat resulted in hypermutation of the *AvrPm8* gene in the powdery mildew pathogen

Lukas Kunz¹ , Alexandros G. Sotiropoulos¹ , Johannes Graf¹ , Mohammad Razavi² , Beat Keller^{1*} and Marion C. Müller^{1,3*}

Abstract

Background Worldwide wheat production is under constant threat by fast-evolving fungal pathogens. In the last decades, wheat breeding for disease resistance heavily relied on the introgression of chromosomal segments from related species as genetic sources of new resistance. The *Pm8* resistance gene against the powdery mildew disease has been introgressed from rye into wheat as part of a large 1BL.1RS chromosomal translocation encompassing multiple disease resistance genes and yield components. Due to its high agronomic value, this translocation has seen continuous global use since the 1960s on large growth areas, even after *Pm8* resistance was overcome by the powdery mildew pathogen. The long-term use of *Pm8* at a global scale provided the unique opportunity to study the consequences of such extensive resistance gene application on pathogen evolution.

Results Using genome-wide association studies in a population of wheat mildew isolates, we identified the avirulence effector *AvrPm8* specifically recognized by *Pm8*. Haplovariant mining in a global mildew population covering all major wheat growing areas of the world revealed 17 virulent haplotypes of the *AvrPm8* gene that grouped into two functional categories. The first one comprised amino acid polymorphisms at a single position along the *AvrPm8* protein, which we confirmed to be crucial for the recognition by *Pm8*. The second category consisted of numerous destructive mutations to the *AvrPm8* open reading frame such as disruptions of the start codon, gene truncations, gene deletions, and interference with mRNA splicing. With the exception of a single, likely ancient, gain-of-virulence mutation found in mildew isolates around the world, all *AvrPm8* virulence haplotypes were found in geographically restricted regions, indicating that they occurred recently as a consequence of the frequent *Pm8* use.

Conclusions In this study, we show that the broad and prolonged use of the *Pm8* gene in wheat production worldwide resulted in a multitude of gain-of-virulence mechanisms affecting the *AvrPm8* gene in the wheat powdery mildew pathogen. Based on our findings, we conclude that both standing genetic variation as well as locally occurring new mutations contributed to the global breakdown of the *Pm8* resistance gene introgression.

Keywords Wheat, Powdery mildew, *Blumeria graminis*, Resistance introgression, Avirulence gene, Gain-of-virulence

*Correspondence:

Beat Keller

bkeller@botinst.uzh.ch

Marion C. Müller

marion.mueller@botinst.uzh.ch; marion.mueller@tum.de

Full list of author information is available at the end of the article



© The Author(s) 2023. **Open Access** This article is licensed under a Creative Commons Attribution 4.0 International License, which permits use, sharing, adaptation, distribution and reproduction in any medium or format, as long as you give appropriate credit to the original author(s) and the source, provide a link to the Creative Commons licence, and indicate if changes were made. The images or other third party material in this article are included in the article's Creative Commons licence, unless indicated otherwise in a credit line to the material. If material is not included in the article's Creative Commons licence and your intended use is not permitted by statutory regulation or exceeds the permitted use, you will need to obtain permission directly from the copyright holder. To view a copy of this licence, visit <http://creativecommons.org/licenses/by/4.0/>. The Creative Commons Public Domain Dedication waiver (<http://creativecommons.org/publicdomain/zero/1.0/>) applies to the data made available in this article, unless otherwise stated in a credit line to the data.

Background

Wheat is one of the most widely cultivated crop species worldwide, serving as an important source of calories and protein for human nutrition [1]. Sustainable wheat production is however threatened by numerous, fast-evolving fungal pathogens. Breeding efforts continuously aim to incorporate new resistance traits into high-yielding cultivars. Since the beginning of the twentieth century, introgressions from closely related wild and domesticated grass species represent one of the most valuable sources for new resistance genes [2]. In the 1930s, the 1RS chromosomal segment of rye (*Secale cereale*) cultivar “Petkus” was introduced into hexaploid wheat, replacing the wheat chromosome arm 1BS [3]. Cultivars carrying the 1BL.1RS translocation not only exhibited higher yield potential but also increased disease resistance against leaf rust, yellow rust, stem rust, and wheat powdery mildew since the rye translocation harbors the *Lr26*, *Yr9*, *Sr31*, and *Pm8* resistance genes [4]. Due to the unique combination of favorable traits, cultivars carrying the 1BL.1RS translocation have been broadly used in wheat growing areas worldwide since the 1960s and continue to be dominantly represented in wheat breeding programs in many countries [5–8]. For example, in 1998, the 1BL.1RS translocation was present in 50% of the high-yielding bread wheat lines from the “International Maize and Wheat Improvement Center (CIMMYT)”, while it reached up to 90% of planted hectareage in some national breeding programs [5, 9, 10]. While the *Sr31* gene remained effective against stem rust for more than 30 years before it was overcome by the highly virulent strain Ug99 [11, 12], the mildew resistance gene *Pm8* broke down quickly in many regions of the world, usually within few years of large-scale deployment of 1BL.1RS cultivars [10, 13–16]. Despite the quick reduction in resistance effectiveness, *Pm8* remained common within the wheat breeding pool, due to complete genetic linkage with the other favorable traits present on the 1BL.1RS translocation [5, 10].

The *Pm8* gene is allelic to *Pm17*, a second rye-derived resistance gene used in wheat breeding and residing on a 1AL.1RS translocation from rye cultivar “Insave” [17]. *Pm8* and *Pm17* encode intracellular, nucleotide-binding leucine-rich repeat (NLR) immune receptors and were found to be homologous to the endogenous wheat *Pm3* resistance locus [17, 18]. The *Pm3* resistance gene codes for numerous, highly similar NLR variants (*Pm3a* to *Pm3t*) [19, 20] that confer resistance against wheat powdery mildew *Blumeria graminis* f. sp. *tritici* (*B.g. tritici*). *Blumeria graminis* (grass powdery mildew) is an obligate biotrophic ascomycete fungus existing in numerous sub-lineages (formae speciales) that exhibit high levels of host specificity, such as *B.g. tritici* exclusively infecting wheat or *B.g. secalis* growing on the *Pm8/Pm17* donor species

rye. The NLR proteins encoded by the *Pm3* allelic series and *Pm17*, where shown to provide race specific resistance against *B.g. tritici* through recognition of mildew encoded effector proteins (avirulence factors, *AVRs*) [21–24]. The *B.g. tritici* avirulence genes *AvrPm3^{a2/f2}*, *AvrPm3^{b2/c2}*, *AvrPm3^{d3}*, and *AvrPm17*, recognized by *Pm3a/Pm3f*, *Pm3b/Pm3c*, *Pm3d*, and *Pm17*, respectively encode highly diverse, small, secreted effector proteins with a common Y/FxC motif and a predicted RNA-se like structure. Population level sequence analysis coupled with functional characterization of gain-of-virulence variants of these *AVRs* has provided a detailed insight into the evolutionary and molecular mechanisms involved in the resistance breakdown of *Pm3* and *Pm17*. For example, gain-of-virulence mutations in the *AvrPm3* and *AvrPm17* effector genes were exclusively found to generate single amino acid polymorphisms, likely allowing *B.g. tritici* to evade NLR recognition while preserving effector virulence function [23–25].

It is estimated that about 5% of modern bread wheat lines harbor a *Pm3* resistance gene [26] and *Pm17* was mostly used in limited geographic regions such as the USA or China [27, 28]. Thus, *Pm8* is by far the most frequently and continuously used powdery mildew resistance gene in wheat breeding and agricultural production of the last decades [5, 9, 10, 18]. The identification of the corresponding avirulence gene *AvrPm8* is therefore of high relevance, as it would provide an unprecedented insight into the consequences of such broad resistance gene application on the global wheat mildew population. Simultaneously, it would allow to better understand the rapid breakdown of *Pm8* resistance that occurred within few years of its deployment and seemingly independently in multiple regions of the world. Such insights would guide more-informed decisions in future resistance breeding, resulting in more durable resistance against the powdery mildew pathogen.

Results

Genome-wide association studies (GWAS) have been previously used to identify avirulence genes in *B.g. tritici* [23, 29]. In order to identify the *AvrPm8* gene, we performed GWAS, using a diversity panel of 79 *B.g. tritici* isolates from a worldwide collection [30] and the chromosome-scale genome assembly of *Pm8* avirulent isolate ISR_7 [24] as a reference (Fig. 1a). Since *Pm8* resistance is largely overcome worldwide, we tailored the *B.g. tritici* diversity panel in order to increase the frequency of avirulent isolates. We did so by including a high proportion of isolates collected in the fertile crescent that were recently shown to exhibit the highest genetic diversity [30]. The GWAS diversity panel was subsequently phenotyped on three *Pm8* containing genotypes: the

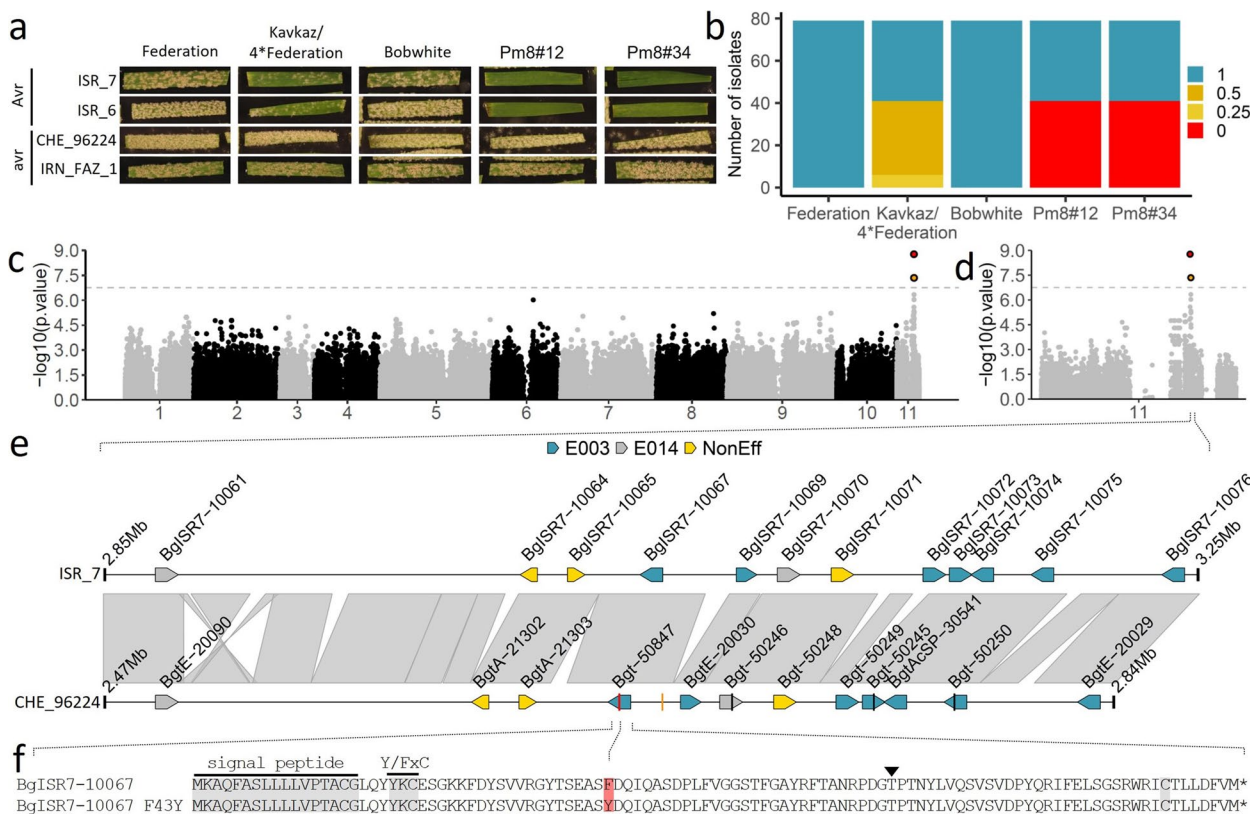


Fig. 1 Identification of *AvrPm8* by GWAS. **a** Representative phenotypic spectrum of two avirulent (*Avr*) and two virulent (*avr*) *B.g. tritici* isolates on *Pm8* wheat lines “Kavkaz/4*Federation” and two independent transgenic lines “Pm8#12” and “Pm8#34”. Susceptible wheat cultivars “Federation” and “Bobwhite” served as controls. **b** Phenotypic distribution of 79 *B.g. tritici* isolates used for GWAS. Leaf coverage (i.e., virulence) was scored 8–10 days after infection using five categories ranging from 0 (0% leaf coverage) to 1 (100% leaf coverage). **c, d** Results of GWAS for avirulence on *Pm8*. Association between sequence polymorphisms and phenotype are depicted along the 11 chromosomes (**c**) or exclusively along chromosome 11 (**d**) of *Pm8* avirulent isolate *ISR_7*. Significance threshold at $p < 0.05$ after Bonferroni correction is indicated as a dashed line. The two significantly associated SNPs on chromosome 11 are highlighted in red (best associated SNP) and yellow. **e** Sequence comparison of the genomic region harboring the *AvrPm8* candidate gene *BgISR7-10067* in the genome assemblies of isolates *ISR_7* (top track) and *CHE_96224* (bottom track). Co-linearity is indicated between the two tracks (gray). Genes are indicated by arrows; gene models are not drawn to scale. Effector genes of effector family E003 (blue), effector family E014 (gray) are highlighted. Non-effector genes are depicted in yellow. The two significantly associated SNPs of the GWAS analysis are indicated by red (best associated SNP) and yellow lines. **f** Sequence alignment of the effector proteins encoded by *AvrPm8* candidate *BgISR7-10067* in *ISR_7* and its orthologous gene *BgISR7-10067_F43Y* (*Bgt-50847*) in *CHE_96224*. Hallmarks of *B.g. tritici* effector proteins such as the predicted signal peptide, the Y/FxC motif and a conserved cysteine at the C-terminus are indicated in gray. The best associated SNP of the GWAS analysis corresponding to the amino acid substitution F43Y is highlighted in red. The black arrowhead indicates the position of the intron

near-isogenic line “Kavkaz/4*Federation,” which is based on one of the earliest released commercial cultivars carrying the 1BL.1RS translocations “Kavkaz,” as well as two independent *Pm8* transgenic lines “Pm8#12” and “Pm8#34” described in [18]. Forty-one isolates, including the reference isolate *ISR_7*, showed an avirulent phenotype on the *Pm8* transgenic lines (i.e., no sporulation) and consistently exhibited reduced but residual sporulation on “Kavkaz/4*Federation” indicating that endogenous expression levels of *Pm8* are not sufficient to provide complete resistance under laboratory conditions (Fig. 1a, b). In contrast, the remaining 38 isolates

exhibited a virulent *Pm8* phenotype, efficiently infecting all three *Pm8*-containing genotypes (Fig. 1a, b). Genomic association between sequence polymorphisms (SNPs) and virulence/avirulence patterns on *Pm8* containing wheat lines identified two significantly associated SNPs, separated by 15,554 bp and mapping to an effector gene cluster on the short arm of *B.g. tritici* chromosome 11 (Fig. 1c–e). Best association was found for snp280882, located within the coding sequence of the *BgISR7-10067* effector gene. *BgISR7-10067* is part of effector gene family E003 (nomenclature of [31]) that also contains the recently identified *AvrPm17* (Fig. 1e, Additional file 1:

Fig. S1) [24]. In a next step, we compared the genomic region harboring *BgISR7-10067* in the *Pm8* avirulent isolate ISR_7 with the corresponding region in the genome assembly of isolate CHE_96224 [31], which exhibits a virulent phenotype on *Pm8* (Fig. 1a). Sequence comparison revealed high levels of co-linearity in this chromosomal region and only minor structural differences that do not affect any coding genes (Fig. 1e). Strikingly, the effector proteins encoded by *AvrPm8* candidate gene *BgISR7-10067* and its orthologous gene in isolate CHE_96224 (*Bgt-50847* according to nomenclature of [31]) differ by a single amino acid polymorphism (F43Y) which corresponds to the best associated SNP snp280882 in the GWAS analysis (Fig. 1e–f). Furthermore, *BgISR7-10067* presents all the hallmarks of avirulence effectors in *B.g. tritici*, such as a small protein size (i.e., 107 amino acids), the presence of a signal peptide, a Y/FxC motif (Fig. 1f), and high expression levels during early infection stages (Additional file 1: Fig. S2a) [22–24, 29, 32]. *BgISR7-10067* was therefore considered an excellent *AvrPm8* candidate gene.

In order to validate *AvrPm8*, we co-expressed *BgISR7-10067* with *Pm8-HA* in *Nicotiana benthamiana* using transient *Agrobacterium* mediated overexpression [23]. To ensure efficient translation in planta, we codon-optimized all fungal effector constructs omitting the predicted signal peptide and fused them to a C-terminal FLAG epitope tag for protein detection by Western blotting. Co-expression of *BgISR7-10067* (hereafter referred to as *AvrPm8*) with *Pm8-HA* resulted in a strong cell-death response (hypersensitive response, HR) in *Nicotiana*, which was absent when either of the components was expressed alone (Fig. 2a, b), confirming

BgISR7-10067 as *AvrPm8*. In agreement with the virulent phenotype of isolate CHE_96224, its orthologous gene *Bgt-50847* (*AvrPm8_F43Y*) did not trigger any HR response upon co-expression with *Pm8* (Fig. 2a–c). Western blot analysis confirmed the efficient production of both FLAG-tagged *AvrPm8* variants and *Pm8-HA* in *N. benthamiana*, indicating the F43Y mutation affects recognition of *AvrPm8* by its cognate immune receptor *Pm8* (Fig. 2d, e).

Given the rye origin of the *Pm8* resistance gene, we searched for *AvrPm8* homologous genes in the rye infecting sublineage of *Blumeria*, *Blumeria graminis* f. sp. *secalis* (*B.g. secalis*). We hypothesized that based on its host range and divergence from *B.g. tritici* approximately 200,000 years ago [33], *B.g. secalis* should have been exposed to the *Pm8* resistance specificity over a longer evolutionary time frame than *B.g. tritici*. In all tested *B.g. secalis* isolates (5), we found an *AvrPm8* homolog (*AvrPm8_Bgs*), encoding for a protein with 13 amino acid differences compared to *AvrPm8* (Fig. 3a). Interestingly, the *AvrPm8* homologous gene in *B.g. secalis* harbored the identical sequence polymorphism found in *B.g. tritici*, leading to the amino acid substitution F43Y. This indicates that the gain-of-virulence substitution F43Y and its underlying DNA polymorphism are relatively ancient. Similar to *AvrPm8_F43Y*, co-expression of *AvrPm8_Bgs* with *Pm8-HA* in *N. benthamiana* did not result in an HR response (Fig. 3b). The efficient production of *AvrPm8_Bgs* protein in *N. benthamiana* (Fig. 3c) indicated that *AvrPm8_Bgs* indeed evades *Pm8* recognition, at least in part due to its F43Y mutation. Consistent with our findings in *N. benthamiana*, *B.g. secalis* isolates exhibited full virulence on *Pm8* containing rye cultivars

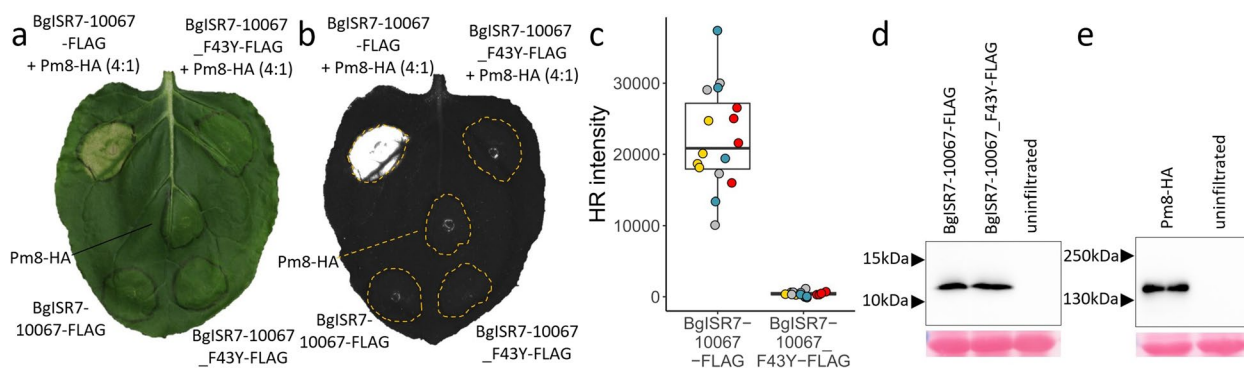


Fig. 2 Functional validation of *AvrPm8* in *Nicotiana benthamiana*. **a, b** *Agrobacterium*-mediated transient expression in *Nicotiana benthamiana* of *BgISR7-10067*-FLAG (*AvrPm8*) or *BgISR7-10067_F43Y*-FLAG (*AvrPm8_F43Y*) co-infiltrated with (top) or without (bottom) *Pm8-HA*. Leaves were imaged at 5 days post inoculation using a normal camera (**a**) or using a Fusion FX imager system (**b**). Co-infiltrations were performed with a ratio of 4 (effector): 1 (*Pm8-HA*). Co-expression of *BgISR7-10067* with *Pm8* resulted in hypersensitive cell-death (HR) in four independent experiments with a total of $n = 16$ leaves. Co-expression of *BgISR7-10067_F43Y* with *Pm8* or expression of any component alone did not result in HR ($n = 16$). **c** Quantification of HR intensity in co-expression assay depicted in **b**. Individual datapoints are color coded based on four independent experiments with $n = 4$ leaves per experiment (total $n = 16$). **d, e** Detection of *N. benthamiana* expressed *AvrPm8*-FLAG and *AvrPm8_F43Y*-FLAG (**d**) or *Pm8-HA* (**e**) by anti-FLAG or anti-HA western blotting (top panel) or total protein Ponceau S staining (bottom panel). Black arrows indicate positions of protein size markers

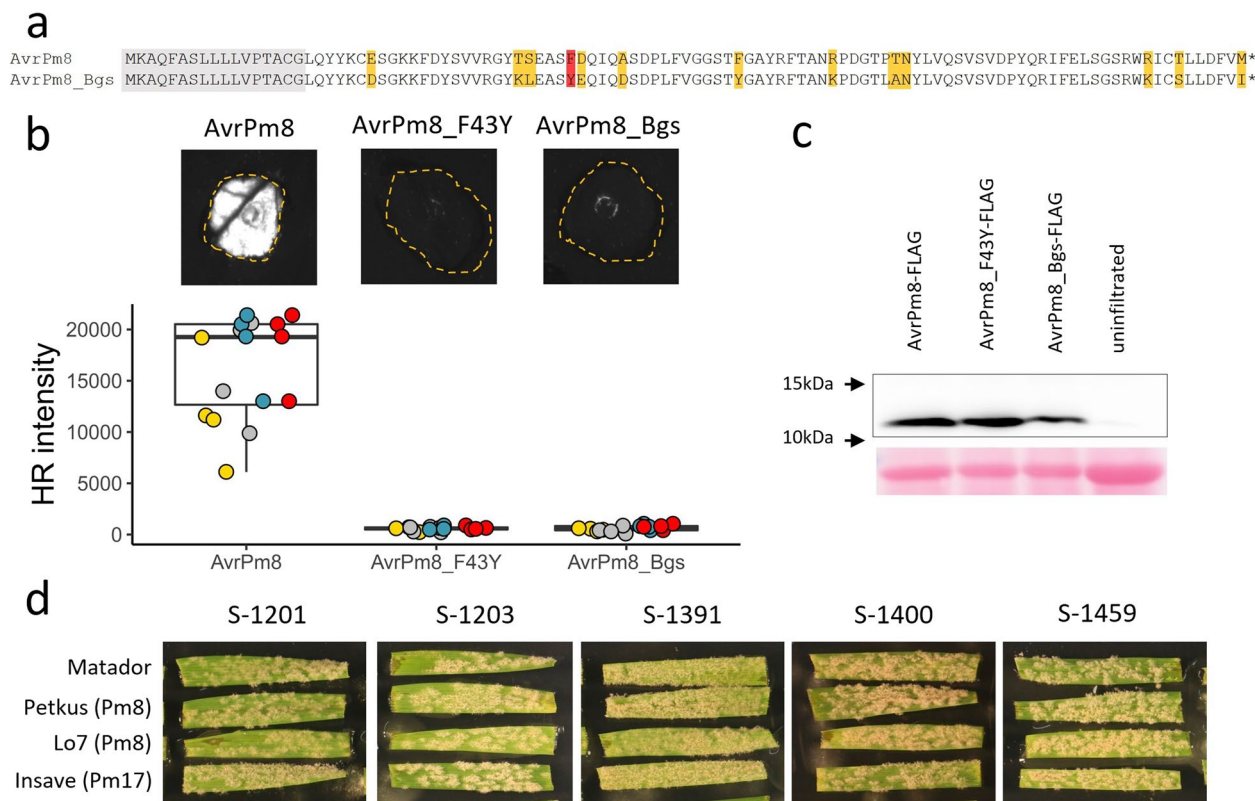


Fig. 3 The *AvrPm8* homologous gene in *B.g. secalis* is not recognized by *Pm8*. **a** Protein sequence alignment of *AvrPm8* and its *B.g. secalis* homolog *AvrPm8_Bgs*. Predicted signal peptide (gray), F43Y substitution (red) and additional polymorphic residues (yellow) are highlighted. **b** *Agrobacterium*-mediated transient co-expression of *AvrPm8*-FLAG, *AvrPm8_F43Y*-FLAG, and *AvrPm8_Bgs*-FLAG with *Pm8*-HA. Leaves were imaged at 5 days post inoculation using a Fusion FX imager system (top panel). Co-infiltrations were performed with a ratio of 4 (effector): 1 (*Pm8*-HA). Bottom panel: quantification of HR intensity in co-expression assay depicted in top panel. Individual datapoints are color coded based on four independent experiments with $n = 4$ leaves per experiment (total $n = 16$). **c** Detection *N. benthamiana* expressed *AvrPm8*-FLAG, *AvrPm8_F43Y*-FLAG, and *AvrPm8_Bgs*-FLAG by anti-FLAG western blotting (top panel) or total protein Ponceau S staining as a loading control (bottom panel). Black arrows indicate positions of protein size markers. **d** Virulence phenotype of five *B.g. secalis* isolates on rye cultivars “Petkus” and “Lo7” both carrying a *Pm8* gene, rye cultivar “Insave” carrying *Pm17* and ‘Matador’ as a susceptible control. Pictures were taken 10 days after infection

“Petkus”, the donor cultivar of the 1BL.1RS translocation [3], and “Lo7” an inbred rye line which was recently shown to contain *Pm8* [34], indicating *AvrPm8_Bgs* represents a true virulence allele (Fig. 3d). To rule out that the observed virulence phenotypes with *AvrPm8_F43Y* in *B.g. tritici* and *AvrPm8_Bgs* in *B.g. secalis* are caused by underlying changes in gene expression, we compared RNA-sequencing data from isolate *ISR_7*, carrying the recognized *AvrPm8*, with five wheat infecting isolates harboring *AvrPm8_F43Y* and two rye infecting isolates carrying *AvrPm8_Bgs*. Both *AvrPm8* virulence alleles exhibited expression levels comparable to *AvrPm8* in *ISR_7* in all tested isolates (Additional file 1: Fig. S2b). These findings further substantiate the importance of the F43Y substitution in *AvrPm8* for the evasion of *Pm8* recognition.

In order to get a more in-depth view on the resistance breakdown of *Pm8* in wheat, we performed extensive

haplotype mining of the *AvrPm8* gene in a global collection of 219 *B.g. tritici* isolates [30]. In addition to the above described *AvrPm8* and *AvrPm8_F43Y* variants, we identified a single synonymous mutation and 17 sequence polymorphisms that impact the open reading frame (ORF) of the *AvrPm8* gene in various ways (Fig. 4a). This included an additional point mutation affecting the crucial amino acid position F43 (F43L) and numerous mutations resulting in a premature stop codon (Q4STOP, K28STOP, D30STOP, S32STOP, L77STOP, R96STOP). Additionally, we identified three independent mutations disrupting the start codon ATG (ATG > GTG, ATG > AAG, ATG > ATC) (Fig. 4a). Furthermore, we identified four independent mutations affecting terminal dinucleotides (i.e., splice acceptor or donor sites) of the single intron found in the *AvrPm8* gene (Fig. 4a). Mutations in the highly conserved terminal dinucleotides (GT-AG) have been found to disrupt mRNA maturation

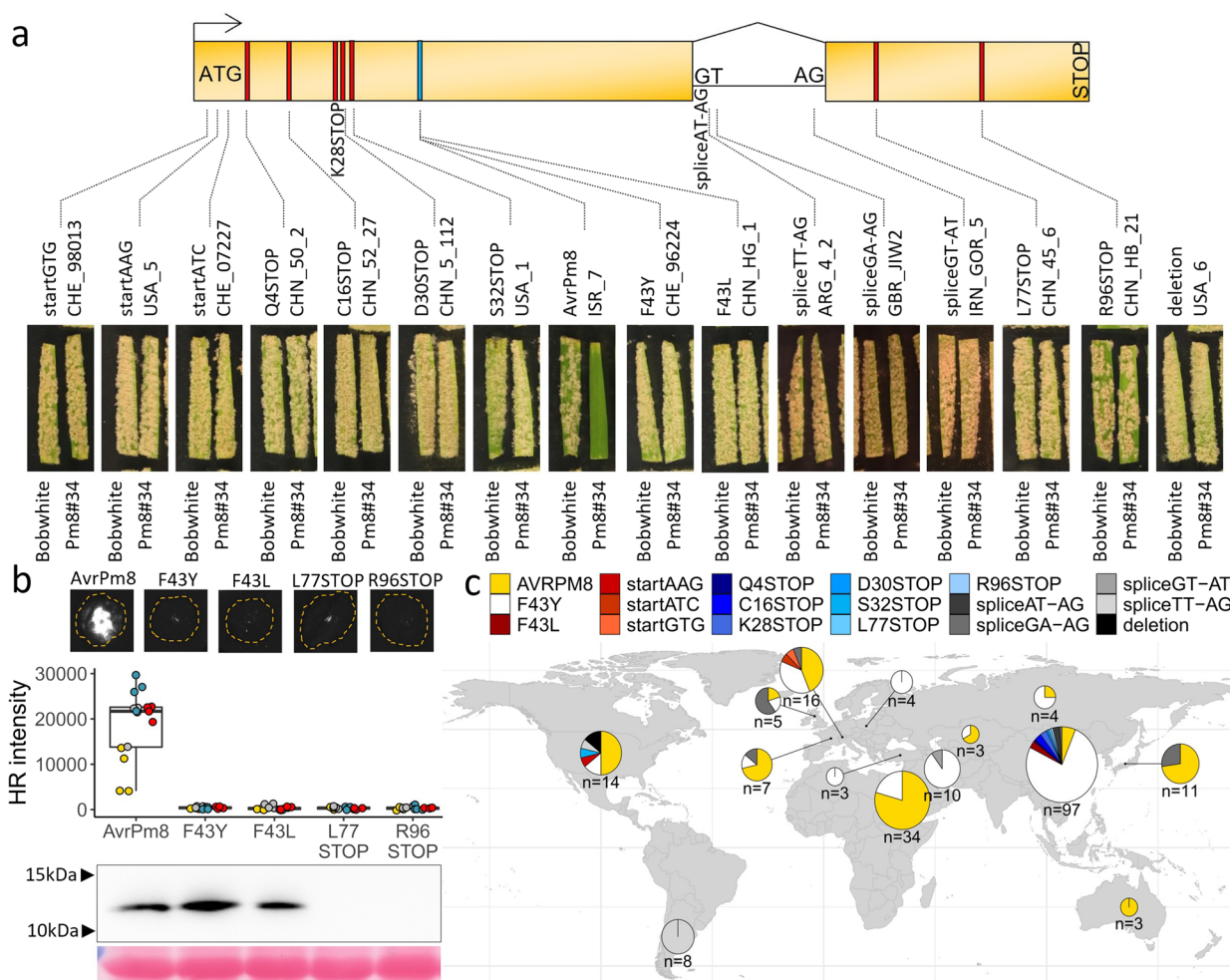


Fig. 4 *AvrPm8* haplovariant mining in a global *B.g. tritici* population reveals 17 gain-of-virulence mutations. **a** Schematic gene model (top) and phenotypes (bottom) of isolates with the identified gain-of-virulence mutations in the *AvrPm8* effector gene. The two exons of *AvrPm8* are depicted as yellow boxes with gene orientation indicated by an arrow. Start codon, splice sites, and stop codon are indicated. Mutations leading to an amino acid change (blue) or a premature stop codon (red) are indicated by a colored line. For each mutation, the virulence phenotype of a representative isolate on the *Pm8* transgenic line Pm8#34 is depicted. Susceptible cultivar “Bobwhite” serves as a control. The phenotype of the avirulent isolate ISR_7 is shown as comparison (middle). Additional phenotyping data for each isolate including phenotypes on the near-isogenic line “Kavkaz/4*Federation” and an independent *Pm8* transgenic line Pm8#12 are depicted in Additional file 1: Fig. S5. For two mutations (K28STOP and spliceAT-AG), we were unable to find a representative isolate in our living *B.g. tritici* collection. **b** *Agrobacterium* mediated co-expression of genes encoding *AvrPm8*-FLAG, *AvrPm8*_F43Y-FLAG, *AvrPm8*_F43L-FLAG, *AvrPm8*-R96STOP-FLAG, or *AvrPm8*-L77STOP-FLAG with *Pm8*-HA in *N. benthamiana*. Leaves were imaged at 5 days post inoculation using a Fusion FX imager system (top panel). Co-infiltrations were performed with a ratio of 4 (effector): 1 (*Pm8*-HA). Middle panel: quantification of HR intensity in co-expression assay depicted in top panel. Individual datapoints are color coded based on four independent experiments with $n = 4$ leaves per experiment (total $n = 16$). Detection of *N. benthamiana* expressed *AvrPm8* constructs by anti-FLAG western blotting (bottom panel) and total protein Ponceau S staining as a loading control. Black arrows indicate positions of protein size markers. **c** Worldwide distribution of identified *AvrPm8* haplovariants. Haplovariants are depicted in different colors according to the legend above the world map. Size of pie charts are scaled as $\log_{10}(n)$ where n is the number of isolates per region

and result in exon skipping or retention of the intron (see Additional file 1: Supplementary Note S1) [35–39]. We hypothesized that the disruption of splicing of the *AvrPm8* mRNA could represent a gain-of-virulence mechanism. Indeed, analysis of RNA sequencing data from GBR_JIW2, an isolate carrying a mutation in the 5' dinucleotide leading to the splice sites GA-AG (instead

of GT-AG), verified the altered *AvrPm8* transcript to be expressed, albeit at lower levels as compared to *Pm8* avirulent isolate ISR_7 (Additional file 1: Fig. S3a), and confirmed splicing of the intron to be largely abolished (Fig. 4a, Additional file 1: Fig. S3b, Supplementary Note S1) [35–39]. Ribosomal translation of unspliced *AvrPm8* mRNA would therefore lead to a premature stop codon

upon translation of the intron and consequentially a truncated protein. In addition to all above-mentioned single nucleotide polymorphisms affecting the *AvrPm8* gene, we also found two independent, large deletion events of 14 and 43 kb, both encompassing the entire *AvrPm8* gene (Fig. 4a, Additional file 1: Fig. S4).

In order to understand the impact of individual mutations found in *AvrPm8*, we tested representative isolates for each mutation on *Pm8* containing wheat lines “Kavkaz/4*Federation” and the two transgenic *Pm8* lines, wherever isolates were available in our living *B.g. tritici* collection (15 out of 17 mutations). For all *AvrPm8* mutations tested, the affected isolates exhibited a fully virulent phenotype on *Pm8* wheat, indicating that all *AvrPm8* haplotypes apart from the ISR7 haplotype, represent virulence alleles (Fig. 4a, Additional file 1: Fig. S5). To verify this finding in *N. benthamiana*, we co-expressed *AvrPm8_F43L*, or the two longest variants with premature stop codons, *AvrPm8_L77STOP* and *AvrPm8_R96STOP*, with *Pm8* in the *Nicotiana* system. Consistent with the phenotype of corresponding isolates on *Pm8* wheat, none of these *AvrPm8* variants was recognized by *Pm8* (Fig. 4b). Western blot analysis revealed efficient production of *AvrPm8_F43L* in *Nicotiana*, further pinpointing at the crucial role of the phenylalanine (F) at position 43 for *Pm8* recognition (Fig. 4b). In contrast, both truncated *AvrPm8* variants (*L77STOP* and *R96STOP*) were undetectable in protein extracts from *Nicotiana*, indicating the truncations result in an unstable *AvrPm8* protein (Fig. 4b). Such instability also has to be assumed for all other premature stop codon inducing mutations (*Q4STOP*, *K28STOP*, *D30STOP*, *S32STOP*), resulting in an even shorter open reading frame.

We then analyzed the worldwide distribution of the avirulent *AvrPm8* variant and any of the above-described gain-of-virulence mutations. Several patterns became apparent. Firstly, the recognized *AvrPm8* variant is found in most subpopulations worldwide (Fig. 4c). Given the fact that *Pm8* resistance is largely broken, *AvrPm8* was surprisingly frequent in populations in Central Europe, the USA, and particularly in Israel, Japan, and Australia (Fig. 4c). While some of these regions suffer from under-sampling and interpretations should be drawn with caution, the dominance of *AvrPm8* in the well-covered Israeli subpopulation is striking. We hypothesize that the Israeli population was exposed to a less severe *Pm8*-dependent selection pressure due to the existence of *Pm8*-free wild wheat progenitors growing naturally in this region. The only virulent variant with worldwide distribution is the *AvrPm8_F43Y* allele. It represents the most common *AvrPm8* haplotype found worldwide and dominates in frequency in many subpopulations on the Eurasian continent and particularly in China (Fig. 4c). Based on its

widespread occurrence and the fact that an identical mutation is found also in *B.g. secalis* (Fig. 3a), we hypothesize that the *AvrPm8_F43Y* virulence allele is ancient and precedes the introgression of *Pm8* into wheat. In contrast to the broadly found *AvrPm8* and *AvrPm8_F43Y* variants, all other *AvrPm8* haplovariants were found only in few isolates often with geographically very restricted occurrence (Fig. 4c). For example, the *AvrPm8_F43L* haplovariant was found exclusively in China, the three identified start codon mutations were found in single isolates either in Switzerland (startGTG, startATC) or the USA (startAAG) and the multiple variants with premature stop codons were unique to China (*Q4STOP*, *K28STOP*, *D30STOP*, *L77STOP*, *R96STOP*) or the USA (*S32STOP*). In particular, the USA and Chinese *B.g. tritici* populations harbored many unique gain-of-virulence mutations of *AvrPm8*. Our findings indicate that, apart from the *F43Y* substitution, gain-of-virulence mutations represent relatively recent events, likely as a consequence of local selection pressure exerted by the high prevalence of *Pm8* wheat.

Discussion

Genomic analyses of *B.g. tritici* and *Blumeria graminis* f. sp. *hordei* (barley powdery mildew) revealed that a high proportion of effector genes encode small, secreted proteins with a predicted RNase-like structure [40–42]. Several RNase-like effectors have furthermore been implicated in virulence processes of *Blumeria* [43–47]. It is therefore not surprising that up to date all identified avirulence proteins in *B.g. tritici* and *B.g. hordei* fall into this effector category. The newly identified *AvrPm8* is no exception to this rule and exhibits common features like small size, presence of a signal peptide, a Y/FxC motif, and a conserved cysteine towards the C-terminus. Like *AvrPm17*, it furthermore belongs to effector family E003, previously shown to contain effectors with a predicted RNase-like structure [24, 48, 49]. The recently identified *AvrPm3^{a2/f2}*, *AvrPm3^{b2/c2}*, *AvrPm3^{d3}*, and *AvrPm17* are recognized by NLRs encoded by the *Pm3* allelic series and the *Pm3* homologous rye NLR *Pm17*, respectively. They all exhibited exceptionally high expression levels during early stages of the infection process, indicating an important function in the establishment of a successful infection [22–24]. Again, *AvrPm8* shows a similar trend by ranking among the 5% highest expressed genes during infection (Additional file 1: Fig. S2a).

Genetic dissection of fungal avirulence on the *Pm3* allelic series revealed significant complexity, involving two genetically unlinked avirulence components for *Pm3a* and *Pm3b* as well as a fungal encoded dominant negative suppressor gene (*SvrPm3*) acting on all tested *Pm3* alleles [22]. In particular, the *SvrPm3* gene

was found to exhibit high levels of expression polymorphisms between fungal isolates, thereby additionally contributing to the complexity of the system [22, 25]. In contrast, our data suggest that the *AvrPm8* gene represents the only fungal component controlling infection outcomes on *Pm8*. Firstly, GWAS analysis using a worldwide diversity panel of 79 wheat powdery isolates identified a single, narrowly defined, genetic association with avirulence on *Pm8* wheat, encompassing a single effector gene subsequently validated as *AvrPm8*. Secondly, across all our phenotypic analyses, we found that all 41 isolates exhibiting an avirulent phenotype on *Pm8* wheat lines are carrying the recognized *AvrPm8* haplotype, whereas all 54 isolates exhibiting a virulent phenotype on *Pm8* contained obvious gain of virulence mutations in the *AvrPm8* locus (Fig. 4a, Additional file 2: Supplementary Dataset S1). Furthermore, transcriptomic analyses indicated that full-length *AvrPm8* haplotypes (i.e., *AvrPm8* and *AvrPm8_F43Y*) are highly expressed during early infection stages in all tested isolates (Additional file 1: Fig. S2b). Taken together, these findings suggest that virulence on *Pm8* is controlled solely by sequence polymorphisms in the fungal *AvrPm8* locus.

Haplotype mining approaches for *AvrPm3* and *AvrPm17* combined with functional characterization of the diverse natural variants have led to a detailed understanding of gain-of-virulence mechanisms and associated resistance breakdown of the *Pm3* allelic series and its rye homolog *Pm17*. Interestingly, *AvrPm3* and *AvrPm17* gain-of-virulence mutations were found to rely on single amino acid polymorphisms and copy number variation in some cases, while preserving at least one functional ORF of the effector gene in each case [23–25]. These findings contrast with gain-of-virulence mutations in recently identified avirulence genes *AvrSr27*, *AvrSr35*, and *AvrSr50* of the biotrophic wheat stem rust pathogen, which frequently involved avirulence gene deletion, transposable element insertion, or drastic expression polymorphisms [38, 50, 51]. The conservation of an intact ORF in virulence alleles of *AvrPm17* and *AvrPm3* genes was interpreted as indications for the counterselection of deleterious mutations due to the importance of the effector function for *B.g. tritici* virulence [23, 24]. Haplotype mining in a worldwide *B.g. tritici* diversity panel for *AvrPm8* also identified two single amino acid polymorphisms leading to gain-of-virulence. Strikingly, the F43Y and F43L mutations affected the same amino acid, indicating an important function of phenylalanine at position 43 for recognition by *Pm8* (Fig. 4a, b). Whether the F43 residue is directly involved in the molecular recognition mechanism of the *Pm8* immune receptor (i.e., direct interaction) and mutations in other residues of the *AvrPm8* protein would less efficiently lead to evasion

of recognition or whether such mutations would be disadvantageous to the pathogens virulence remains to be determined. The presence of 12 additional amino acid polymorphisms in the *AvrPm8* homolog found in *B.g. secalis* (Fig. 3a) indicates that polymorphisms throughout the *AvrPm8* protein can be tolerated. It is possible that missense mutations in other regions of the *AvrPm8* protein would result in only partial gain-of-virulence phenotypes on *Pm8* which, due to the broad application of *Pm8*, would be quickly outcompeted by fully virulent *AvrPm8* haplotypes. Indeed, partial virulence phenomena have been observed for several naturally occurring amino acid polymorphisms in the closely related *AvrPm17* [24]. We hypothesize that expanding haplotype mining efforts would reveal additional amino acid polymorphisms, even though they might be less frequent as compared to the *AvrPm3s* and *AvrPm17*.

In contrast to the conservation of intact open reading frames in *AvrPm3* and *AvrPm17* virulence alleles, we found strong convergent evolutionary trends for the occurrence of more drastic virulence mutations to the *AvrPm8* gene. Not only did we find evidence for numerous independent mutation events affecting the same structural components of the *AvrPm8* gene such as the start codon or splice sites but also most of the identified gain-of-virulence mutations lead to significant truncations or the complete destruction of the *AvrPm8* ORF. Strikingly, the natural diversity of *AvrPm8* virulence alleles found in the worldwide *B.g. tritici* population strongly resembled the outcome of an artificial EMS mutagenesis screen for gain-of-virulence in *AvrSr35*, which identified 15 virulence inducing mutations involving premature stop codons (12), splice site mutations (1), and two independent mutations affecting the same amino acid [38]. Even though the virulence function of the *AvrPm8* effector is currently unknown, given the frequency of deleterious mutations to the *AvrPm8* ORF under natural conditions, we hypothesize that *AvrPm8* effector activity, in contrast to *AvrPm17* and *AvrPm3* effectors, is dispensable without major fitness costs in *B.g. tritici*. We therefore argue that the diverse deterioration of the *AvrPm8* gene observed in *B.g. tritici* is a consequence of the dispensability of *AvrPm8* effector function in combination with the strong selection pressure exerted by the broad and frequent use of the *Pm8* resistance gene as part of the 1BL.1RS translocation in wheat.

The deployment of 1BL.1RS wheat cultivars in larger agricultural settings was first reported in 1960s followed by its integration into national and international breeding programs and associated increase in planted acreage in the following decades [5–8]. In many countries, the *Pm8* resistance breakdown was however reported within few years of 1BL.1RS deployment [10, 13–16]. Given

the broad application and reported near-complete *Pm8* breakdown, we were surprised by the prevalence of the avirulent *AvrPm8* haplovariant in specific local *B.g. tritici* populations such as Australia, Israel, Japan, or Central Europe. We hypothesize that this reflects consequences of local breeding decisions (i.e., low frequency of *Pm8* cultivars) or, in the case of Israel, the availability of sympatrically growing, *Pm8*-free, wild wheat relatives such as wild emmer known to allow growth of *B.g. tritici* [52] that could have served as sanctuary host populations leading to a reduced *Pm8* selection pressure in this region.

Interestingly, we found only a single virulence allele, *AvrPm8_F43Y* with worldwide occurrence. Its widespread distribution and the presence of an identical nucleotide polymorphism in the related *B.g. secalis* sublineage suggests the F43Y mutation is ancient and likely precedes *Pm8* introgression from rye to wheat. This is reminiscent of the ancient genetic variation identified in *AvrPm17*, including multiple gain-of-virulence mutations, explaining the quick breakdown of the *Pm17* resistance gene introgressed into wheat [24]. Interestingly *AvrPm8_F43Y* dominated *B.g. tritici* population in many regions where the 1BL.1RS translocation dominantly impacted local breeding programs, and the *Pm8* resistance was reported to be completely broken, such as Eastern Europe and in particular China [5, 7, 10, 28]. Especially the Chinese *B.g. tritici* subpopulation analyzed in this study exhibited striking patterns of a strong selection for virulence on *Pm8* lines consistent with previous reports [7, 28]. Among the 97 analyzed isolates, only six carried the avirulent *AvrPm8* haplovariant, with the remaining isolates carrying either *AvrPm8_F43Y* (74) or one of eight locally occurring gain-of-virulence variants. The near complete absence of the avirulent *AvrPm8* is reminiscent of a recent study in a global population of Septoria leaf blotch which found absence of avirulent forms of *AvrStb6* in modern Septoria isolates due to widespread use of *Stb6* wheat in recent years [53]. The Chinese *B.g. tritici* population furthermore exemplifies the observed global trend for rare, locally restricted gain-of-virulence innovations that are represented by mostly deleterious mutations to the *AvrPm8* open reading frame. Based on their restricted distribution, we hypothesize that these *AvrPm8* virulence variants represent recent mutational events that occurred and propagated locally upon exposure of a *B.g. tritici* subpopulation to *Pm8*.

It has been assumed that the near simultaneous breakdown of powdery mildew resistance genes such as *Pm17* or *Pm8* in wheat growing areas worldwide can, at least partially, be explained by the ability of powdery mildew ascospores to travel large distances within only few growing seasons thereby allowing the efficient spread of new gain-of-virulence alleles [54, 55]. However, a recent

population genomics analysis by Sotiropoulos et al. [30], making use of the same *B.g. tritici* diversity panel used for this study, found strong associations between genetic proximity and geographic origin and convincingly attributed the exchange of mildew genetic material over long distances (i.e., continents) to human activities in historic times followed by hybridization events. These findings are consistent with our hypothesis of frequent, locally restricted de novo gain-of-virulence mutations in *AvrPm8* leading to the seemingly simultaneous breakdown of *Pm8* resistance worldwide.

The quick breakdown of *Pm8* by convergent evolution in powdery mildew contrasts the breakdown of the more durable *Sr31* resistance gene residing on the same 1BL.1RS rye translocation. Even though the underlying resistance mechanism of *Sr31* is not known, the emergence of the *Sr31* virulent race Ug99 in Uganda could be attributed to a single evolutionary event involving nuclear exchange during somatic hybridization [56] and subsequent stepwise spread of the Ug99 lineage to countries in Africa and the Middle East [11]. The differences in the breakdown of *Pm8* and *Sr31* exemplify the different evolutionary dynamics involved in resistance gene breakdown, likely influenced not only by the molecular mode of action of the resistance gene but also by the importance of the underlying virulence functions of the recognized fungal effector as well as the lifestyles, genetic diversity, and genome stability of the involved fungal pathogens. We therefore consider it crucial to expand the study of fungal avirulence gene dynamics in various wheat pathogens in order to understand emerging patterns of resistance gene breakdown and consequently allow informed breeding decisions towards more durable resistance.

Conclusions

The identification of the wheat mildew avirulence effector *AvrPm8* and extensive haplovariant mining efforts in a worldwide wheat mildew collection allowed to reconstruct the breakdown of *Pm8* resistance in wheat. We conclude that the quick and seemingly simultaneous breakdown of *Pm8* worldwide was caused by a combination of (i) the widespread presence of an ancient gain-of-virulence mutation in *AvrPm8*, likely preceding *Pm8* introgression into wheat, and (ii) the frequent local occurrence of deleterious mutations affecting the *AvrPm8* gene as a consequence of the extreme selection pressure exerted by the ubiquitous *Pm8* genotypes. Our study exemplifies the consequences of broad and prolonged resistance gene use on avirulence gene diversity in fast evolving fungal plant pathogens such as wheat powdery mildew. Our findings furthermore highlight the importance to expand our understanding of

fungal avirulence gene dynamics in the future in order to achieve more durable genetic resistance against plant pathogens.

Methods

Plant material, fungal isolates, and virulence phenotyping

The “Kavkaz/4*Federation” *Pm8* near-isogenic line has been previously described in [18]. The two independent *Pm8* transgenic lines carrying the complete genomic sequence of the *Pm8* resistance gene under a maize ubiquitin promoter have been selected as best performing lines in the study of [18]. The *Pm8* rye cultivar “Petkus,” serving as the original donor for 1BL.1RS translocation in wheat, and the inbred rye line “Lo7” have been previously shown to contain the *Pm8* resistance gene [18, 34]. The rye cultivar “Insave” carrying the *Pm17* resistance gene has been described in [17].

Information about the collection of 219 *B.g. tritici*, 2 *B.g. triticales*, and 5 *B.g. secalis* isolates is summarized in Supplementary Dataset S1 (Additional file 2) and, with the exception of 10 newly sequenced Iranian isolates as part of this study, is described in great detail in [30]. *B.g. tritici* and *B.g. triticales* isolates were maintained clonally on leaf segments of susceptible bread wheat cultivar “Kanzler”. *B.g. secalis* isolates were maintained clonally on leaf segments of susceptible rye cultivar “Matador”. For fungal propagation, detached leaves were placed on 0.5% food grade agar (PanReac AppliChem) plates containing 4.23mM benzimidazole [57].

For *B.g. tritici* and *B.g. triticales* isolates *Pm8* virulence phenotypes were assessed on the near-isogenic line ‘Kavkaz/4*Federation’ and two independent *Pm8* transgenic lines Pm8#12 and Pm8#34 [18] with the susceptible control “Federation” and “Bobwhite,” respectively. For *B.g. secalis* isolates, virulence phenotypes were assessed on rye cultivars “Petkus” and “Lo7” (both with *Pm8*), “Insave” (*Pm17*) and on the susceptible control “Matador”. Virulence scoring at 8–10 days after infection was performed on at least three biological replicates and based on qualitative assessment of mildew leaf coverage (MLC) in five categories: virulent (V): 100% MLC; intermediate/virulent (I/V): 75% MLC; intermediate (I): 50% MLC; avirulent/intermediate (A/I): 25% MLC; avirulent (A): 0% MLC. Virulence scoring was performed on non-blinded samples. Phenotyping results are summarized in Supplementary Dataset S1 (Additional file 2). For the depiction of virulence phenotypes throughout the manuscript, representative images were chosen.

Bioinformatic datasets

The chromosome-scale assembly of isolate CHE_96224 (*Bgt_genome_v3_16*) is described in [31]. The genome

assembly of ISR_7 is described in [24]. To resolve the chromosomes of the ISR_7 genome, the contigs of the ISR_7 assembly (available at the European nucleotide archive under accession number CAKMHR020000001 - CAKMHR020000032) were aligned against *Bgt_genome_v3_16* using blastn [58] and ordered according to the best blasthit (first criterium: evaluate, second criterium: bitscore). The ordered assembly was subsequently polished using Illumina reads of ISR_7 previously published (SRA: SRX1140177, [33]). First, Illumina reads were quality trimmed using sickle (v1.33, <https://github.com/najos/sickle>) with options: pe -q 33 -l 40 and then aligned to the ISR_7 assembly using bowtie2 with the following parameters: -score-min L,-0.6,-0.25 (v2.3.4.1, [59]). Mappings files were processed with SAMtools (v1.7, [60]) sort, view, and rmdup commands followed by Picards (<https://broadinstitute.github.io/picard/>) AddOrReplaceReadGroups command. Assembly polishing was done with pilon (v1.23, [61]) with the -fix bases option. The final chromosome assembly is available at ENA accession number: PRJEB41382.

To create a draft annotation of the ISR_7 assembly, maker (v2.31.10, [62]) was used with prot2genome option based on proteins of CHE_96224 (version *Bgt_CDS_v4_23*, available at <https://zenodo.org/record/7018501>) with repeat masking of the maker internal TE proteins, as well as the PTREP_2019 and nrTREP_2019 databases (available at <https://trep-db.uzh.ch/>). Subsequently, above-described steps were repeated with protein sequences from *B. g. hordei* isolates DH14 and RACE1 (GCA_900239735.1, GCA_900237765.1). Gene models from the second round were only added if the identified loci did not contain a gene model from the first round of annotation. The resulting draft annotation file is available at <https://zenodo.org/record/6998719>.

Whole-genome resequencing datasets used in this study have been described in [30] unless indicated otherwise. Isolation, DNA extraction and sequencing of the 10 Iranian *B.g. tritici* strains newly described in this study was achieved as described by [30]. All whole-genome resequencing datasets are available from the SRA under project numbers indicated in Supplementary Dataset S1 (Additional file 2).

Raw RNA-sequencing reads of *B.g. tritici* isolates CHE_96224, CHE_94202, and GBR_JIW2 infecting wheat cultivar “Chinese Spring,” *B.g. triticales* isolates THUN-12 and T3-8 infecting triticales cultivar “Timbo” and *B.g. secalis* isolates S-1391 and S-1459 infecting rye cultivar “Matador”, at 2 days post infection (2dpi) are available at sequence read archive (SRA) under accession number PRJNA427159 [63]. RNA-sequencing reads of *B.g. tritici* isolates ISR_7 and CHN_17-40 infecting wheat cultivar “Chinese Spring” at 2dpi were produced

as described in [63] and sequenced on a NovaSeq, PE150 with 12Gb/20M reads total data output for each of three biological replicates (available from SRA under accession number PRJNA870298 and PRJNA904717, respectively).

Expression analysis

Expression analysis of *ISR_7* was performed using salmon (v0.7.2 [64]). First, CDS file of *ISR_7* (available at <https://zenodo.org/record/6998719>) was indexed using the salmon index command. Subsequently, read counts per gene were calculated with the salmon quant command. Then, count data was normalized using the calcNormFactors (method="TMM") command from edgeR package (v3.38.4, [65]), and rpkm values per gene were calculated using the rpkm() command. Gene expression of all expressed genes (average rpkm value of three replicates >0) was plotted with a custom R script available at <https://github.com/MarionCMueller/AvrPm8>. For *AvrPm8* expression analysis in different isolates, RNA sequencing reads from selected isolates (see methods section "Bioinformatic datasets") were processed with the pipeline described above for *ISR_7*. The custom R script to generate the plot is available at <https://github.com/MarionCMueller/AvrPm8>.

Genome-wide association studies (GWAS)

For GWAS analysis, Illumina sequences of the 79 isolates (as indicated in Additional file 2: Supplemental Dataset S1) were mapped against the *ISR_7* genome assembly. First, sequences were quality trimmed using Trimmomatic (v0.38, [66]) option LEADING:3 TRAILING 3 SLIDING WINDOW:4:20 MINLEN:50. Next, paired reads were aligned to *ISR_7* assembly using bowtie2 (v2.2.9, [59]) with parameters `-score-min L,-0.6,-0.25`. Files were subsequently processed with SAMtools view, sort, and rmdup commands (v1.6, [60]). Finally, files were processed using Picard (<https://broadinstitute.github.io/picard/>) with the ADDORREplaceREADGroups command. SNPcall was performed with freebayes (v1.1.0-54-g49413aa, <https://github.com/freebayes/freebayes>) with `-genotype quality` and `-p 1` options. The resulting vcf was filtered using vcfutils (v0.1.5, [67]) with the following parameters: `--maf 0.05, --max-alleles 2 --min-alleles 2 --minDP10 --minGQ 40 --minQ 40 --max-missing 1 --remove-indels`. The filtered vcf file was transformed to hapmap format using a custom perl script. GWAS was performed using phenotypic data from *Pm8* transgenic lines Pm8#12 and Pm8#34 with GAPIT3 ([68]) using the following options: `PCA.total=3, Model.selection=TRUE, model="GLM", kinship.algorithm="VanRanden"`. Scripts and dataset used to run the GWAS analysis are available at (<https://github.com/MarionCMueller/AvrPm8>).

github.com/MarionCMueller/AvrPm8). Manhattan plots were visualized with a custom R script available at <https://github.com/MarionCMueller/AvrPm8>.

AvrPm8 haplotype mining

For *AvrPm8* haplotype mining, whole-genome resequencing datasets were mapped to the *B.g. tritici* reference assembly of CHE_96224 (Bgt_genome_v3_16, [31]) using bwa (0.7.17-r1188, [69]) as described in [30] and visualized using the integrative genomics viewer IGV (v2.8.6 [70]). *AvrPm8* haplotypes were defined by manual inspection for each isolate.

Analysis of *AvrPm8* splicing

To analyze splicing of the *AvrPm8* mRNA, RNA-sequencing reads of isolates *ISR_7* and *GBR_JIW2* were aligned to the genome assembly of *ISR_7* using STAR (v2.5.3, [71]) as follows: first, an index of the genome was created using the `--genomeGenerate` command. Secondly, RNAseq reads were aligned to the genome assembly with options `--alignIntronMax 500, --outFilterMultimapNmax 5, --outFilterMismatchNoverLmax 0.04 --outSAMtype BAM SortedByCoordinate`. The resulting .bam files of three biological replicates were merged using the BamTools merge command (v2.5.1, <https://github.com/pezmaster31/bamtools>). Merged .bam-files were indexed using the SAMtools index command (v1.6, r [60]) and visualized using the integrative genomics viewer (IGV) (v2.8.10, [70]).

Comparative genomics analysis of the *AvrPm8* locus

To analyze co-linearity of the *AvrPm8* locus between the two genome assemblies of *ISR_7* and CHE_96224, the Chr-11 of both genome assemblies was compared using the nucmer command of the MUMmer program (v4.0.0rc1, [72]). Subsequently the generated delta file was processed with the dnadiff command of the MUMmer suite. The resulting file out.lcoords was visualized in R studio using the gggenomes package (<https://github.com/thackl/gggenomes>). Gene models in the locus were quality controlled manually, gene models that were erroneous or were not supported by RNA-seq reads were not depicted. Scripts and input files used to generate Fig. 1e are available at Github (<https://github.com/MarionCMueller/AvrPm8>).

Phylogenetic tree

To define E003 effector family members in *ISR_7*, protein sequences of E003 family members of *B.g. tritici* reference isolates Bgt_96224 [24] were blasted against the protein sequences of *ISR_7* (available at <https://zenodo.org/record/6998719>) using the blastp command from

BLAST+ v2.6.0+, [58] with *e*-value cutoff of $10e-50$. Protein sequences were aligned using muscle algorithm implemented in MEGA-X software (v10.0.5, [73]). The sequence of BgtE-20002 (AVRPMB2/C2) was used as an outgroup. The phylogenetic tree was constructed using FastTree software (v2.1.11, [74]) with default parameters. FigTree (v1.4.4, <https://github.com/rambaut/figtree/releases/tag/v1.4.4>) was used to visualize the tree. Protein sequences of E003 family members and the raw tree file is available at (<https://github.com/MarionCMueller/AvrPm8>).

Verification of *AvrPm8* deletion by PCR

The extent of the *AvrPm8* gene deletion in USA_6 and USA_Ken_4_3 was estimated based on whole-genome resequencing data (see *AvrPm8* haplotype mining). For each deletion, a primer pair flanking the possibly deleted region was designed (for primer sequences see Additional file 1: Supplementary Table S1). Genomic DNA was extracted from fungal spores using the chloroform and CTAB based extraction procedure described by [22]. PCR amplification spanning the gene deletion was achieved using Phusion High-Fidelity DNA Polymerase (New England Biolabs) according to the manufacturers protocol and visualized on a 1% agarose gel supplied with ethidium bromide.

Cloning of expression constructs

A gateway system compatible entry clone carrying the entire *Pm8* genomic sequence fused to a C-terminal Myc-tag (pENTR-*Pm8*-myc) has been described by [75]. For this study, the myc-epitope tag was replaced by a hemagglutinin (HA) epitope (creating pENTR-*Pm8*-HA) by PCR based site-directed mutagenesis (SDM) using non-overlapping primers listed in Supplementary Table S1 (Additional file 1) and Phusion High-Fidelity DNA Polymerase (New England Biolabs). Subsequently, the linear PCR product was phosphorylated using T4 polynucleotide kinase (New England Biolabs) and ligated with T4 DNA Ligase (New England Biolabs) according to the manufacturer.

The coding sequence, omitting the signal peptide as predicted by SignalP4.0 [76], of all *AvrPm8* effector variants was codon-optimized for *N. benthamiana* using the tool provided by Integrated DNA technologies (<https://eu.idtdna.com>), C-terminally fused to a FLAG epitope tag, and synthesized with gateway compatible attL sites by our commercial partner BioCat GmbH (<https://www.biocat.com>). Sequence information of all constructs produced by gene synthesis can be found in Supplementary Dataset S2 (Additional file 3).

All gateway compatible entry clones described above were mobilized into the binary expression vector pIPKb004 [77] using Gateway LR clonase II (Invitrogen) according to the manufacturer and subsequently transformed into *Agrobacterium tumefaciens* strain GV3101 using a freeze-thaw transformation protocol [78].

Avr-R co-expression and HR quantification in *N. benthamiana*

Agrobacterium tumefaciens mediated expression of resistance and effector genes was achieved following the detailed protocol of [23]. For co-expression, *Agrobacteria* carrying the effector or resistance gene were mixed in a ratio of 4:1 directly prior to infiltration. HR development was assessed 4–5 days after infiltration using a Fusion FX imaging System (Vilber Lourmat, Eberhardzell, Germany) and quantified using Fiji [79] as described by [23]. For the depiction of HR phenotypes throughout the manuscript, representative images were chosen. Each co-expression experiment was performed individually 4 times on 4 individual *N. benthamiana* plants each, resulting in a total of $n = 16$ leaves for HR quantification.

Western blotting

To test for protein production in *N. benthamiana*, single constructs were expressed as described above and infiltrated plant tissue harvested 2 days after *Agrobacterium* infiltration. Protein extraction was achieved as described in [23]. Protein extracts were separated on homemade 4–20% gradient SDS polyacrylamide gels and blotted to a nitrocellulose membrane (Amersham Protran 0.2 μ m NC) using a Trans-Blot SD Semi-Dry Transfer Cell (BioRad). Blotting efficiency was assessed by staining total protein with Ponceau S. For the detection of *Pm8*-HA, anti-HA-HRP antibody (rat monoclonal, clone 3F10, Roche) was used at a dilution of 1:3000. For detection of FLAG tagged *AvrPm8* variants, anti-FLAG-M2-HRP (mouse monoclonal, clone M2, Sigma-Aldrich) was used at a dilution of 1:3000. Peroxidase chemiluminescence was detected using a Fusion FX imaging System (Vilber Lourmat, Eberhardzell, Germany) and SuperSignal West Femto HRP substrate (Thermo Scientific) for FLAG tagged effectors or WesternBright ECL HRP substrate (Advansta) for *Pm8*-HA. For each western blot analysis reported, protein expression, extraction, and western blotting was conducted a total of 3 times with similar results. Uncropped western blots are depicted in Additional file 4.

Supplementary Information

The online version contains supplementary material available at <https://doi.org/10.1186/s12915-023-01513-5>.

Additional file 1: Figure S1. Phylogenetic analysis of effector family E003 in *B.g. tritici* isolate ISR_7. **Figure S2.** *AvrPm8* (*BglSR7-10067*) is highly expressed in *Blumeria graminis* isolates. **Figure S3.** Splice site mutations in isolate GBR_JIW2 abolish splicing of *AvrPm8* (*BglSR7-10067*). **Figure S4.** Isolates USA_6 and USA_Ken-4-3 carry independent gene deletions that encompass the *AvrPm8* gene. **Figure S5.** *AvrPm8* mutations result in gain-of-virulence phenotypes on *Pm8* wheat. **Note S1.** Splice site mutations. **Table S1.** List of primers used in this study.

Additional file 2: Supplementary Dataset S1. Summary of *Blumeria graminis* isolates used in this study.

Additional file 3: Supplementary Dataset S2. List and sequence of gene synthesis constructs used in this study.

Additional file 4. Uncropped Western blots for Figs. 2d, e, 3c and 4b.

Acknowledgements

We would like to thank Andres Gordillo from KWS Saat SE & Co for providing the “Lo7” seeds. We thank Helen Zbinden and Esther Jung for the maintenance of powdery mildew isolates.

Research on plants

This research complies with the relevant institutional, national, and international guidelines and legislation on conducting research on plants.

Authors' contributions

L.K., M.C.M. and B.K. designed the research. L.K., M.C.M. and B.K. wrote the manuscript. L.K. performed the experiments. M.C.M., L.K., A.G.S. and J.G. performed bioinformatic analyses. L.K. and M.C.M. analyzed data. M.R. collected mildew isolates. All authors read and approved the final manuscript.

Funding

This study was supported by Swiss National Science Foundation grants 310030B_182833 and 310030_204165 to BK and the University Research Priority Program (URPP) ‘Evolution in Action’ of the University of Zurich.

Availability of data and materials

Illumina sequences used in this study are available at the short read archive under accession number PRJNA290428 [80] and PRJNA625429 [81]. RNA-sequencing reads are available under accession number PRJNA427159 [82], PRJNA870298 [83], and PRJNA904717 [84]. Genome assembly and annotation of CHE_96224 and assembly of ISR_7 are available under European nucleotide archive (ENA) accession number PRJEB28180 [85] and PRJEB41382 [86], respectively. Annotation and assembly of CHE_96224 are also available from <https://doi.org/10.5281/zenodo.7018501> [87]. Draft annotation of ISR_7 is available at <https://zenodo.org/record/6998719> [88]. Scripts used to produce the figures are available at <https://github.com/MarionCMueller/AvrPm8> [89].

Declarations

Ethics approval and consent to participate

Not applicable.

Consent for publication

Not applicable.

Competing interests

The authors declare that they have no competing interests.

Author details

¹Department of Plant and Microbial Biology, University of Zurich, Zurich, Switzerland. ²Iranian Research Institute of Plant Protection, Agricultural Research, Education and Extension Organization, Tehran, Iran. ³Chair of Phytopathology, TUM School of Life Sciences, Technical University of Munich, Freising, Germany.

Received: 16 September 2022 Accepted: 11 January 2023

Published online: 08 February 2023

References

- FAO. World food and agriculture – statistical yearbook 2021. Rome: Food and Agriculture Organization of the United Nations (FAO); 2021. <https://doi.org/10.4060/cb4477en>, <https://www.fao.org/documents/card/en/c/cb4477en/>.
- Wulff BB, Moscou MJ. Strategies for transferring resistance into wheat: from wide crosses to GM cassettes. *Front Plant Sci.* 2014;5:692.
- Lein A. Introgression of a rye chromosome to wheat strains by Georg Riebesel – Salzmünde after 1926. In: Proceedings of the international symposium on triticales: studies and breeding: 1973. Gatersleben: EUCARPIA; 1975. p. 158–68.
- Crespo-Herrera LA, Garkava-Gustavsson L, Ahman I. A systematic review of rye (*Secale cereale* L.) as a source of resistance to pathogens and pests in wheat (*Triticum aestivum* L.). *Hereditas.* 2017;154:1–9.
- Rabinovich SV. Importance of wheat-rye translocations for breeding modern cultivars of *Triticum aestivum* L. *Euphytica.* 1998;100(1-3):323–40 (Reprinted from *Wheat: Prospects for global improvement*, 1998).
- Graybosch RA. Uneasy unions: quality effects of rye chromatin transfers to wheat. *J Cereal Sci.* 2001;33(1):3–16.
- Zhou Y, He ZH, Sui XX, Xia XC, Zhang XK, Zhang GS. Genetic improvement of grain yield and associated traits in the Northern China winter wheat region from 1960 to 2000. *Crop Sci.* 2007;47(1):245–53.
- Lukaszewski AJ. Frequency of 1RS.1AL and 1RS.1BL translocations in United-States wheats. *Crop Sci.* 1990;30(5):1151–3.
- Villareal RL, Banuelos O, Mujeeb-Kazi A, Rajaram S. Agronomic performance of chromosomes 1B and T1BL.1RS near-isolines in the spring bread wheat Seri M82. *Euphytica.* 1998;103(2):195–202.
- Purnhauser L, Bona L, Lang L. Occurrence of 1BL.1RS wheat-rye chromosome translocation and of Sr36/Pm6 resistance gene cluster in wheat cultivars registered in Hungary. *Euphytica.* 2011;179(2):287–95.
- Singh RP, Hodson DP, Huerta-Espino J, Jin Y, Bhavani S, Njau P, et al. The emergence of Ug99 races of the stem rust fungus is a threat to world wheat production. *Annu Rev Phytopathol.* 2011;49:465–81.
- Pretorius ZA, Singh RP, Wagoire WW, Payne TS. Detection of virulence to wheat stem rust resistance gene Sr31 in *Puccinia graminis* f. sp. *tritici* in Uganda. *Plant Dis.* 2000;84(2):203.
- Bennett FGA. Resistance to powdery mildew in wheat - a review of its use in agriculture and breeding programs. *Plant Pathol.* 1984;33(3):279–300.
- Heun M, Friebe B. Introgression of powdery mildew resistance from rye into wheat. *Phytopathology.* 1990;80(3):242–5.
- Namuco LO, Coffman WR, Bergstrom GC, Sorrells ME. Virulence spectrum of the *Erysiphe graminis* f. sp. *tritici* population in New York. *Plant Dis.* 1987;71(6):539–41.
- Streckeisen PF, P.M. Virulence analysis of powdery mildew of wheat in Switzerland 1981–1983. *Schweizerische-landwirtschaftliche-Forschung.* 1985;24(3-4):261–9 [German].
- Singh SP, Hurni S, Ruinelli M, Brunner S, Sánchez-Martín J, Krukowski P, et al. Evolutionary divergence of the rye *Pm17* and *Pm8* resistance genes reveals ancient diversity. *Plant Mol Biol.* 2018;98(3):249–60.
- Hurni S, Brunner S, Buchmann G, Herren G, Jordan T, Krukowski P, et al. Rye *Pm8* and wheat *Pm3* are orthologous genes and show evolutionary conservation of resistance function against powdery mildew. *Plant J.* 2013;76(6):957–69.
- Yahiaoui N, Srichumpa P, Dudler R, Keller B. Genome analysis at different ploidy levels allows cloning of the powdery mildew resistance gene *Pm3b* from hexaploid wheat. *Plant J.* 2004;37(4):528–38.
- Bhullar NK, Street K, Mackay M, Yahiaoui N, Keller B. Unlocking wheat genetic resources for the molecular identification of previously undescribed functional alleles at the *Pm3* resistance locus. *Proc Natl Acad Sci U S A.* 2009;106(23):9519–24.
- Brunner S, Hurni S, Streckeisen P, Mayr G, Albrecht M, Yahiaoui N, et al. Intragenic allele pyramiding combines different specificities of wheat *Pm3* resistance alleles. *Plant J.* 2010;64(3):433–45.
- Bourras S, McNally KE, Ben-David R, Parlange F, Roffler S, Praz CR, et al. Multiple avirulence loci and allele-specific effector recognition control

- the Pm3 race-specific resistance of wheat to powdery mildew. *Plant Cell*. 2015;27(10):2991–3012.
23. Bourras S, Kunz L, Xue M, Praz CR, Muller MC, Kalin C, et al. The AvrPm3-Pm3 effector-NLR interactions control both race-specific resistance and host-specificity of cereal mildews on wheat. *Nat Commun*. 2019;10(1):2292.
 24. Müller MC, Kunz L, Schudel S, Lawson AW, Kammerecker S, Isaksson J, et al. Ancient variation of the AvrPm17 gene in powdery mildew limits the effectiveness of the introgressed rye Pm17 resistance gene in wheat. *Proc Natl Acad Sci U S A*. 2022;119(30):e2108808119.
 25. McNally KE, Menardo F, Luthi L, Praz CR, Muller MC, Kunz L, et al. Distinct domains of the AVRPM3(A2/F2) avirulence protein from wheat powdery mildew are involved in immune receptor recognition and putative effector function. *New Phytol*. 2018;218(2):681–95.
 26. Bhullar NK, Zhang ZQ, Wicker T, Keller B. Wheat gene bank accessions as a source of new alleles of the powdery mildew resistance gene *Pm3*: a large scale allele mining project. *BMC Plant Biol*. 2010;10:88.
 27. Graybosch R, Bai G, Amand PS, Sarath G. Persistence of rye (*Secale cereale* L.) chromosome arm 1RS in wheat (*Triticum aestivum* L.) breeding programs of the Great Plains of North America. *Genet Resour Crop Evol*. 2019;66(4):941–50.
 28. Zeng F-s, Yang L-j, Gong S-j, Zhang X-j, Wang H, Xiang L-b, et al. Virulence and diversity of *Blumeria graminis* f. sp. *tritici* populations in China. *J Integr Agr*. 2014;13(11):2424–37.
 29. Praz CR, Bourras S, Zeng FS, Sanchez-Martin J, Menardo F, Xue MF, et al. *AvrPm2* encodes an RNase-like avirulence effector which is conserved in the two different specialized forms of wheat and rye powdery mildew fungus. *New Phytol*. 2017;213(3):1301–14.
 30. Sotiropoulos AG, Arango-Isaza E, Ban T, Barbieri C, Bourras S, Cowger C, et al. Global genomic analyses of wheat powdery mildew reveal association of pathogen spread with historical human migration and trade. *Nat Commun*. 2022;13(1):4315.
 31. Müller MC, Praz CR, Sotiropoulos AG, Menardo F, Kunz L, Schudel S, et al. A chromosome-scale genome assembly reveals a highly dynamic effector repertoire of wheat powdery mildew. *New Phytol*. 2019;221(4):2176–89.
 32. Hewitt T, Müller MC, Molnár I, Mascher M, Holušová K, Šimková H, et al. A highly differentiated region of wheat chromosome 7AL encodes a *Pm1a* immune receptor that recognises its corresponding *AvrPm1a* effector from *Blumeria graminis*. *New Phytol*. 2020;229(5):2812–26.
 33. Menardo F, Praz CR, Wyder S, Ben-David R, Bourras S, Matsumae H, et al. Hybridization of powdery mildew strains gives rise to pathogens on novel agricultural crop species. *Nat Genet*. 2016;48(2):201–5.
 34. Rabanus-Wallace MT, Hackauf B, Mascher M, Lux T, Wicker T, Gundlach H, et al. Chromosome-scale genome assembly provides insights into rye biology, evolution and agronomic potential. *Nat Genet*. 2021;53:564–73.
 35. Collins L, Penny D. Complex spliceosomal organization ancestral to extant eukaryotes. *Mol Biol Evol*. 2005;22(4):1053–66.
 36. Frey K, Pucker B. Animal, fungi, and plant genome sequences harbor different non-canonical splice sites. *Cells*. 2020;9(2):458.
 37. Abramowicz A, Gos M. Splicing mutations in human genetic disorders: examples, detection, and confirmation. *J Appl Genet*. 2018;59(3):253–68.
 38. Salcedo A, Rutter W, Wang SC, Akhunova A, Bolus S, Chao SM, et al. Variation in the *AvrSr35* gene determines *Sr35* resistance against wheat stem rust race Ug99. *Science*. 2017;358(6370):1604–6.
 39. He F, Jacobson A. Nonsense-mediated mRNA decay: degradation of defective transcripts is only part of the story. *Annu Rev Genet*. 2015;49:339–66.
 40. Pedersen C, van Themaat EVL, McGuffin LJ, Abbott JC, Burgis TA, Barton G, et al. Structure and evolution of barley powdery mildew effector candidates. *BMC Genomics*. 2012;13:694.
 41. Menardo F, Praz CR, Wicker T, Keller B. Rapid turnover of effectors in grass powdery mildew (*Blumeria graminis*). *BMC Evol Biol*. 2017;17:223.
 42. Seong K, Krasileva KV. Prediction of effector protein structures from fungal phytopathogens enables evolutionary analyses. *Nat Microbiol*. 2023;8:174–87.
 43. Pennington HG, Jones R, Kwon S, Bonciani G, Thieron H, Chandler T, et al. The fungal ribonuclease-like effector protein CSEP0064/BEC1054 represses plant immunity and interferes with degradation of host ribosomal RNA. *PLoS Pathog*. 2019;15(3):e1007620.
 44. Ahmed AA, Pedersen C, Schultz-Larsen T, Kwaaitaal M, Jorgensen HJL, Thordal-Christensen H. The barley powdery mildew candidate secreted effector protein CSEP0105 inhibits the chaperone activity of a small heat shock protein. *Plant Physiol*. 2015;168(1):321–U576.
 45. Ahmed AA, Pedersen C, Thordal-Christensen H. The barley powdery mildew effector candidates CSEP0081 and CSEP0254 promote fungal infection success. *PLoS One*. 2016;11(6):e0157586.
 46. Zhang W-J, Pedersen C, Kwaaitaal M, Gregersen PL, Morch SM, Hanisch S, et al. Interaction of barley powdery mildew effector candidate CSEP0055 with the defence protein PR17c. *Mol Plant Pathol*. 2012;13(9):1110–9.
 47. Pliego C, Nowara D, Bonciani G, Gheorghie DM, Xu R, Surana P, et al. Host-induced gene silencing in barley powdery mildew reveals a class of ribonuclease-like effectors. *Mol Plant Microbe Interact*. 2013;26(6):633–42.
 48. Saur IML, Bauer S, Kracher B, Lu XL, Franzeskakis L, Muller MC, et al. Multiple pairs of allelic MLA immune receptor-powdery mildew AVR(A) effectors argue for a direct recognition mechanism. *Elife*. 2019;8:e44471.
 49. Bauer S, Yu D, Lawson AW, Saur IML, Frantzeskakis L, Kracher B, et al. The leucine-rich repeats in allelic barley MLA immune receptors define specificity towards sequence-unrelated powdery mildew avirulence effectors with a predicted common RNase-like fold. *PLoS Pathog*. 2021;17(2):e1009223.
 50. Chen JP, Upadhyaya NM, Ortiz D, Sperschneider J, Li F, Bouton C, et al. Loss of *AvrSr50* by somatic exchange in stem rust leads to virulence for *Sr50* resistance in wheat. *Science*. 2017;358(6370):1607–10.
 51. Upadhyaya NM, Mago R, Panwar V, Hewitt T, Luo M, Chen J, et al. Genomics accelerated isolation of a new stem rust avirulence gene-wheat resistance gene pair. *Nat Plants*. 2021;7(9):1220–8.
 52. Ben-David R, Parks R, Dinooor A, Kosman E, Wicker T, Keller B, et al. Differentiation among *Blumeria graminis* f. sp. *tritici* isolates originating from wild versus domesticated triticum species in Israel. *Phytopathology*. 2016;106(8):861–70.
 53. Stephens C, Olmez F, Blyth H, McDonald M, Bansal A, Turgay EB, et al. Remarkable recent changes in the genetic diversity of the avirulence gene *AvrStb6* in global populations of the wheat pathogen *Zymoseptoria tritici*. *Mol Plant Pathol*. 2021;22(9):1121–33.
 54. McDonald BA, Linde C. The population genetics of plant pathogens and breeding strategies for durable resistance. *Euphytica*. 2002;124(2):163–80.
 55. Limpert E, Godet F, Muller K. Dispersal of cereal mildews across Europe. *Agric For Meteorol*. 1999;97(4):293–308.
 56. Li F, Upadhyaya NM, Sperschneider J, Matny O, Nguyen-Phuc H, Mago R, et al. Emergence of the Ug99 lineage of the wheat stem rust pathogen through somatic hybridisation. *Nat Commun*. 2019;10(1):5068.
 57. Parlange F, Oberhaensli S, Breen J, Platzer M, Taudien S, Simkova H, et al. A major invasion of transposable elements accounts for the large size of the *Blumeria graminis* f. sp. *tritici* genome. *Funct Integr Genomics*. 2011;11(4):671–7.
 58. Camacho C, Coulouris G, Avagyan V, Ma N, Papadopoulos J, Bealer K, et al. BLAST plus: architecture and applications. *BMC Bioinformatics*. 2009;10:421.
 59. Langmead B, Salzberg SL. Fast gapped-read alignment with Bowtie 2. *Nat Methods*. 2012;9(4):357–9.
 60. Li H, Handsaker B, Wysoker A, Fennell T, Ruan J, Homer N, et al. The sequence alignment/map format and SAMtools. *Bioinformatics*. 2009;25(16):2078–9.
 61. Walker BJ, Abeel T, Shea T, Priest M, Abouelliel A, Sakthikumar S, et al. Pilon: an integrated tool for comprehensive microbial variant detection and genome assembly improvement. *PLoS One*. 2014;9(11):e112963.
 62. Cantarel BL, Korfi I, Robb SMC, Parra G, Ross E, Moore B, et al. MAKER: an easy-to-use annotation pipeline designed for emerging model organism genomes. *Genome Res*. 2008;18(1):188–96.
 63. Praz CR, Menardo F, Robinson MD, Muller MC, Wicker T, Bourras S, et al. Non-parent of origin expression of numerous effector genes indicates a role of gene regulation in host adaptation of the hybrid triticale powdery mildew pathogen. *Front Plant Sci*. 2018;9:49.
 64. Patro R, Duggal G, Love MI, Irizarry RA, Kingsford C. Salmon provides fast and bias-aware quantification of transcript expression. *Nat Methods*. 2017;14(4):417–9.
 65. Robinson MD, McCarthy DJ, Smyth GK. edgeR: a Bioconductor package for differential expression analysis of digital gene expression data. *Bioinformatics*. 2010;26(1):139–40.

66. Bolger AM, Lohse M, Usadel B. Trimmomatic: a flexible trimmer for Illumina sequence data. *Bioinformatics*. 2014;30(15):2114–20.
67. Danecek P, Auton A, Abecasis G, Albers CA, Banks E, DePristo MA, et al. The variant call format and VCFtools. *Bioinformatics*. 2011;27(15):2156–8.
68. Wang J, Zhang Z. GAPIT Version 3: boosting power and accuracy for genomic association and prediction. *Genomics Proteomics Bioinformatics*. 2021;19(4):629–40.
69. Li H, Durbin R. Fast and accurate short read alignment with Burrows-Wheeler transform. *Bioinformatics*. 2009;25(14):1754–60.
70. Robinson JT, Thorvaldsdottir H, Winckler W, Guttman M, Lander ES, Getz G, et al. Integrative genomics viewer. *Nat Biotechnol*. 2011;29(1):24–6.
71. Dobin A, Davis CA, Schlesinger F, Drenkow J, Zaleski C, Jha S, et al. STAR: ultrafast universal RNA-seq aligner. *Bioinformatics*. 2013;29(1):15–21.
72. Marçais G, Delcher AL, Phillippy AM, Coston R, Salzberg SL, Zimin A. MUMmer4: a fast and versatile genome alignment system. *PLoS Comput Biol*. 2018;14(1):e1005944.
73. Kumar S, Stecher G, Li M, Knyaz C, Tamura K. MEGA X: molecular evolutionary genetics analysis across computing platforms. *Mol Biol Evol*. 2018;35(6):1547–9.
74. Price MN, Dehal PS, Arkin AP. FastTree 2—Approximately Maximum-Likelihood trees for large alignments. *PLoS One*. 2010;5(3):e9490.
75. Hurni S, Brunner S, Stirnweis D, Herren G, Peditto D, McIntosh RA, et al. The powdery mildew resistance gene Pm8 derived from rye is suppressed by its wheat ortholog Pm3. *Plant J*. 2014;79(6):904–13.
76. Petersen TN, Brunak S, von Heijne G, Nielsen H. SignalP 4.0: discriminating signal peptides from transmembrane regions. *Nat Methods*. 2011;8(10):785–6.
77. Himmelbach A, Zierold U, Hensel G, et al. A set of modular binary vectors for transformation of cereals. *Plant Physiol*. 2007;145(4):1192–200.
78. Weigel D, Glazebrook J. Transformation of agrobacterium using the freeze-thaw method. *CSH Protoc*. 2006;2006(7):pdb.prot4666.
79. Schindelin J, Arganda-Carreras I, Frise E, Kaynig V, Longair M, Pietzsch T, et al. Fiji: an open-source platform for biological-image analysis. *Nat Methods*. 2012;9(7):676–82.
80. Raw sequence reads of cereal powdery mildew (*Blumeria graminis*) specialized on different hosts. NCBI. 2022. <https://www.ncbi.nlm.nih.gov/bioproject/PRJNA290428>.
81. Raw sequence reads of *Blumeria graminis* f. sp. *tritici/dicocci* from around the world. NCBI. 2022. <https://www.ncbi.nlm.nih.gov/bioproject/PRJNA625429>.
82. Transcriptomics study of three *Blumeria graminis* formae speciales. NCBI. 2022. <https://www.ncbi.nlm.nih.gov/bioproject/PRJNA427159>.
83. RNA-sequencing of *Blumeria graminis* f.sp. *tritici* isolate ISR_7. NCBI. 2022. <https://www.ncbi.nlm.nih.gov/bioproject/PRJNA870298>.
84. RNA-sequencing of *Blumeria graminis* f.sp. *tritici* isolate CHN_17_40. NCBI. 2022. <https://www.ncbi.nlm.nih.gov/bioproject/PRJNA904717>.
85. Müller MC, Praz CR, Sotiropoulos AG, Menardo F, Kunz L, Schudel S, et al. Bgt_genome_v3.16 assembly for *Blumeria graminis* f. sp. *tritici*. ENA. 2022. <https://www.ebi.ac.uk/ena/browser/view/PRJEB28180>.
86. Kunz L, Graf J, Müller MC, Sotiropoulos AG, Keller B. Bgt_ISR7_genome_v1_4 assembly for *Blumeria graminis* f. sp. *tritici*. ENA. 2022. <https://www.ebi.ac.uk/ena/browser/view/PRJEB41382>.
87. Müller MC, Graf J, Keller B. Genome and annotation files (v4_23) for *Blumeria graminis* f. sp. *tritici* isolate CHE_96224 (genome assembly: Bgt_genome_v3_16). Zenodo. <https://doi.org/10.5281/zenodo.7018501>.
88. Kunz L, Graf J, Müller MC, Sotiropoulos AG, Keller B. Genome and annotation files for *Blumeria graminis* f. sp. *tritici* isolate ISR_7 (genome assembly: Bgt_ISR7_genome_v1_4). Zenodo. v1. <https://doi.org/10.5281/zenodo.6998719>.
89. Kunz L, Sotiropoulos AG, Graf J, Razavi M, Keller B, Müller MC. Scripts for AvrPm8 manuscript. Github. 2022. <https://github.com/MarionCMueller/AvrPm8>.

Publisher's Note

Springer Nature remains neutral with regard to jurisdictional claims in published maps and institutional affiliations.

Ready to submit your research? Choose BMC and benefit from:

- fast, convenient online submission
- thorough peer review by experienced researchers in your field
- rapid publication on acceptance
- support for research data, including large and complex data types
- gold Open Access which fosters wider collaboration and increased citations
- maximum visibility for your research: over 100M website views per year

At BMC, research is always in progress.

Learn more biomedcentral.com/submissions

